Robust 1550-nm single-frequency all-fiber ns-pulsed fiber amplifier for wind-turbine predictive control by wind lidar

F. Beier[1], O. de Vries[2], T. Schreiber[2], R. Eberhardt[2] and A. Tünnermann[1,2]
[1] Institute of Applied Physics, Albert-Einstein-Straße 15, 07745 Jena
[2] Fraunhofer Institute for Applied Optics and Precision Engineering, Albert-Einstein-Str. 7, 07745 Jena, Germany

C. Bollig, P. G. Hofmeister, J. Schmidt and R. Reuter
Institute of Physics, Carl von Ossietzky University Oldenburg, 26111 Oldenburg, Germany

ABSTRACT

Scaling of the power yield of offshore wind farms relies on the capacity of the individual wind turbines. This results in a trend to very large rotor diameters, which are difficult to control. It is crucial to monitor the inhomogeneous wind field in front of the wind turbines at different distances to ensure reliable operation and a long lifetime at high output levels. In this contribution, we demonstrate an all-fiber ns-pulsed fiber amplifier based on cost-efficient commercially available components. The amplifier is a suitable source for coherent Doppler lidar pulses making a predictive control of the turbine operation feasible.

Keywords: wind turbine control, coherent lidar, fiber amplifier, stimulated Brillouin scattering

1. INTRODUCTION

The disastrous incidents of Chernobyl in 1986 and most recently at Fukushima Daiichi nuclear power plant caused a worldwide rethinking of the necessity of a sufficient amount of nonpolluting and particularly safe renewable energy sources. The environment-friendly utilization of wind power belongs to this category. Clustered in wind farms, today's wind turbines produce Megawatt-level output powers [1]. To reach the ambitious and politically motivated aims of Multi-GW offshore wind farms - capable of substituting several nuclear power plants - not only the number of turbines in a wind park but the yield of the individual turbine has to be scaled as well. However, growing rotor diameters and the influence of a complex inflow within the rotor area make it more and more difficult to control and operate the wind energy converters. It is therefore crucial to monitor the inhomogeneous wind field in front of the system at different distances to ensure a stable operation as well as a long lifetime at high output levels.

In this contribution, we demonstrate an all-fiber ~250ns-pulsed 1550nm fiber amplifier suitable for coherent Doppler lidar (**li**ght **d**etection **a**nd **r**anging) making a predictive control of the turbine operational parameters feasible. Since this laser should be cost-efficient and suitable for industrialization, all components have to be commercially available. Furthermore, experimental results obtained with two different pumping schemes (co- vs. counter-propagation) and other design criteria such as the efficiency and nonlinear power limitations are discussed. Future power scaling toward 100 µJ, ideal packaging and issues of mechanical and thermal robustness are presented.

2. EXPERIMENTAL SETUP

The experimental setup is based on a silica all fiber amplifier containing two amplifier stages. To examine the physical limits concerning Stimulated Brillouin Scattering (SBS), two concepts of pumping the main amplifier are used. As shown in Fig. 1, a continuous-wave single-frequency (linewidth < 4 kHz FWHM) single-mode diode laser source at 1550 nm is modulated by a radio-frequency driven acousto-optic modulator (AOM) to provide the temporal pulse shape of the signal. It is seeded into a double pass pre-amplifier, consisting of an Er-doped 8 µm core single clad fiber, which is pumped by a 100 mW single-mode laser diode at 976 nm wavelength. Pump and signal are separated by a WDM. The reflection for the second amplification pass is achieved by using a fiber Bragg grating (FBG) with a spectral bandwidth of approximately 1 nm wavelength, minimizing amplified spontaneous emission. As illustrated in Figs. 1 and 2, the signal passes a fiber coupled splitter. At this 10 percent monitor output the temporal behavior of the pulses leaving the preamp is examined.

In the main amplifier stage the pump power is coupled into an Erbium- and Ytterbium-doped double clad fiber with a 10 µm signal core, roughly a length of 3.4 m and 125 µm pump core by a multimode pump coupler in co-propagation mode and alternatively in counter propagation mode. In co-propagating configuration, the seed signal is coupled to the active fiber by using the single mode core of the pump coupler fiber. We use a co-propagating pumping scheme. A short piece of passive SM28 fiber is spliced to the end of the active fiber, which terminates in an angle polished FC/APC connector.
As opposed to this, the signal is coupled directly into the active fiber and the pump light on the opposite side by the pump coupler in the second configuration shown in Fig. 2. The amplified pulses are transmitted through the pump coupler, which is terminated by an angle-polished connector, to be analyzed by a power meter and in addition by a photo diode detector. The fiber optical splitter at the output port of the circulator allows the backscattered SBS pulses to be measured and characterized.

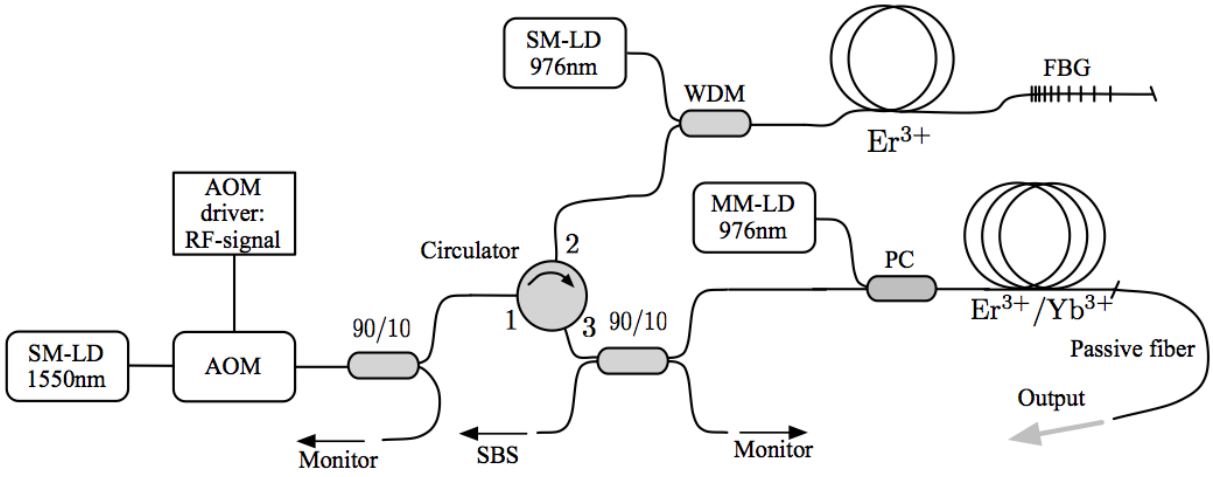

Fig. 1 Experimental setup of the co-propagation mode amplifier system, consisting of two amplification stages. The main amplifier is set up in a co-propagating configuration. The pump and the signal radiation are propagating in the same direction. By using the coupler ports and measuring the transmitted power, the SBS threshold and the pulse variation can be determined.

By comparing the SBS-threshold and the efficiency of the two concepts, the difference can be assessed with respect to the suitability for Doppler lidar systems. For each configuration, several pulse durations and pulse repetition rates between 5 and 50 kHz are investigated. In consideration of the amplifier gain, a higher repetition frequency leads to a decreasing pulse peak power and therefore to a higher average power SBS threshold.

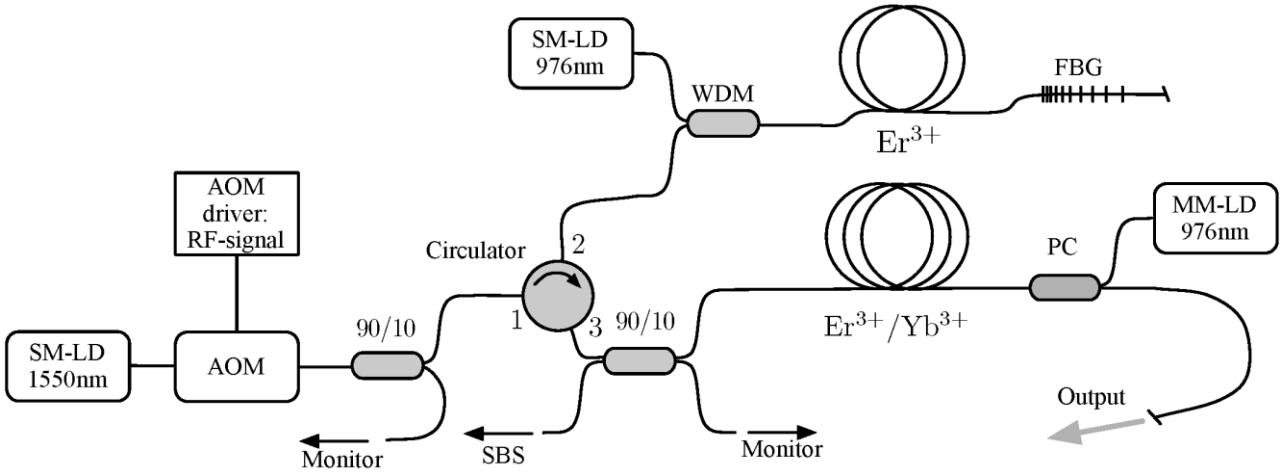

Fig. 2 Experimental setup of the counter-propagation mode amplifier system consisting of two amplification stages. The main amplifier is set up in a counter-propagating configuration. The pump and the signal light are propagating in opposite directions. By using the coupler ports and measuring the transmitted power, the SBS threshold and the pulse variation are determined.

3. EXPERIMENTAL RESULTS

To evaluate the influence of the amplifier configuration to the average output power and the limitations caused by nonlinear effects [2], a 220 ns Full Width Half Maximum (FWHM) pulse at a repetition frequency of 10 kHz is amplified in the co- and the counter-propagation mode. The amplified pulses typically have a pulse length of ~220 ns. In Figs. 3 and 4 the amplifier slopes and the mean backscattered power are shown. Comparing the graphs, a slope efficiency of 17.8% for co-propagation and 25.7% for counter-propagation can be observed.

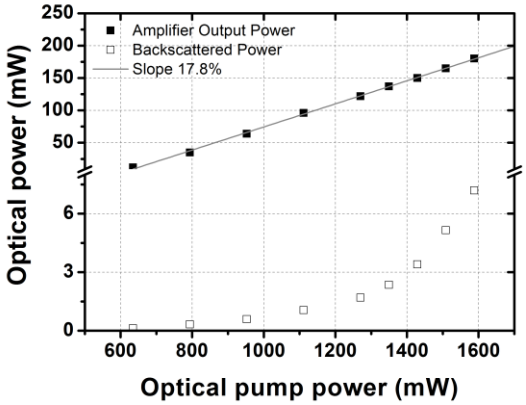

Fig. 3 Optical output power and power of the backscattered light in average concerning the co-propagation amplifier at 220 ns pulse duration and 10 kHz repetition rate.

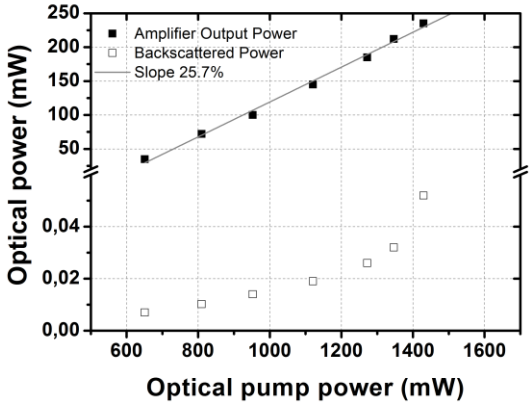

Fig. 4 Optical output power and power of the backscattered light in average concerning the counter-propagation amplifier at 220 ns pulse duration and 10 kHz repetition rate.

Additionally, the power value at the highest pump power level shown in both graphs, corresponds to the limit at which the outgoing pulse is significantly deformed by the loss caused by SBS, as shown in Fig. 5. The power of the backscattered light also increases when the pump power is rising. Up to a level of 1.3 W it shows a linear behavior with respect to the pump power and corresponds to increasing amplified spontaneous emission (ASE). After reaching the SBS threshold, pulses can be seen at the detector in the 10% channel of the optical splitter and the backscattered power rises exponentially. Variations of the backscattered power are caused by the difference in amplification and ASE behavior of the considered setups. Comparing the average output powers at a pump power of 1.3 W, the achievable peak power of the pulses in the counter-propagating amplifier exceeds the power observed in the co-propagating case.

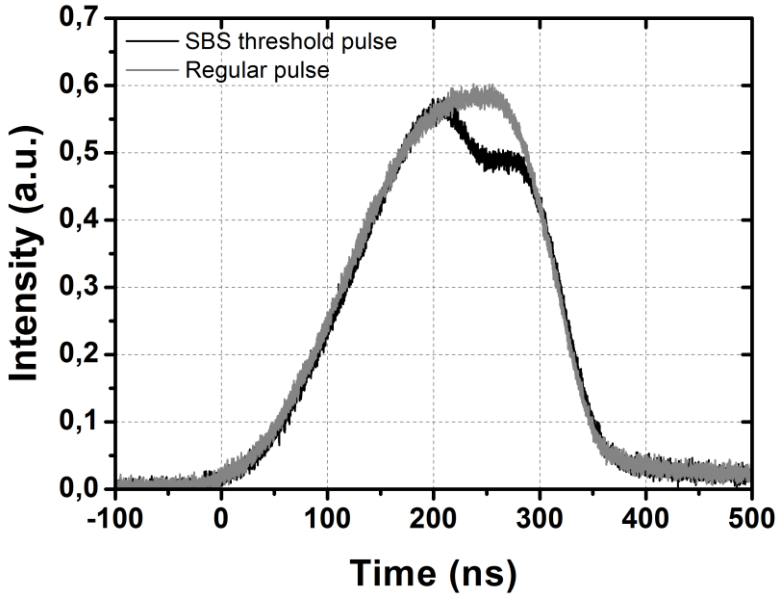

Fig. 5 When the pulse peak power exceeds the SBS threshold, the pulse decreases significantly.

The Figs. 6 and 7 show the behavior of the threshold at different repetition rates, while the pulse duration is maintained. The peak power and the average power are represented regarding the varied pulse repetition frequencies. It is evident that the threshold is higher at the analyzed frequencies in counter-propagating mode.

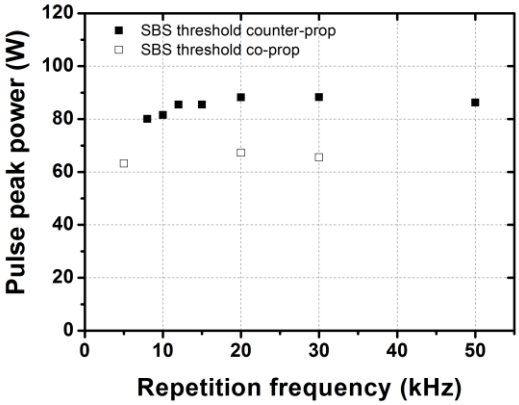

Fig. 6 At a pulse duration of 220 ns a difference in the SBS threshold concerning the pulse peak power can be determined for the various amplifier configurations.

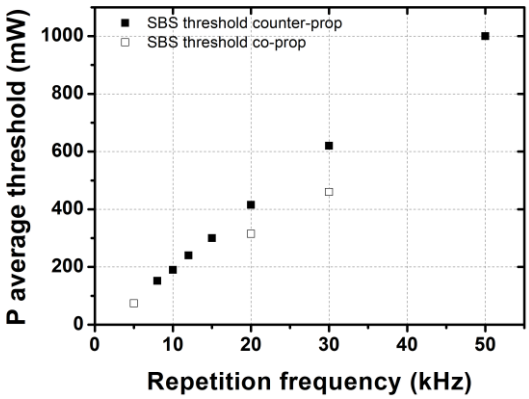

Fig. 7 At a pulse duration of 220 ns a difference in the SBS threshold concerning the average output power can be determined for the various amplifier configurations.

Due to this fact and because of the higher slope efficiency only the counter-propagation system will be discussed in the following. The influence of the pulse duration on the SBS threshold can be determined by setting several repetition frequencies and raising the pump power up to the SBS threshold. The increasing of the fitted lines of the data in Fig. 8 corresponds to the pulse energy of the average pulse at the analyzed pulse durations and results in the following values:

Pulse duration (ns)	Pulse energy SBS thr. (µJ)	Pulse peak power SBS thr. (W)
100	14	131
220	20	86
480	42	82

Enhancement of the SBS threshold depends essentially on the spectral broadening of the signal, which is caused by the limitation in the time domain [3]. By spectral broadening of the signal the SBS gain is reduced. At this point, a spectral analysis of the pulses would be of interest.

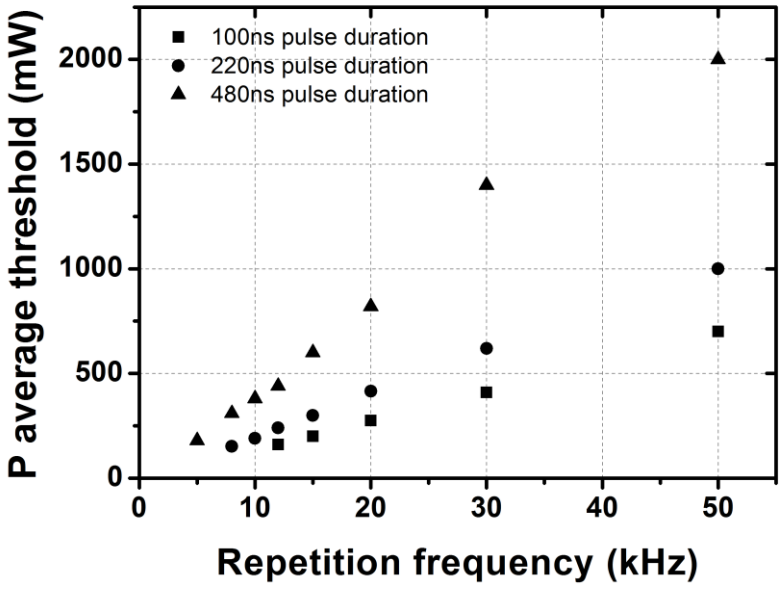

Fig. 8 Measured average power thresholds of SBS depending on the pulse duration.

Besides the shown laser performance there is another crucial issue worthy of attention. Since the laser shall be operated under extreme conditions in terms of mechanical stress and stress attributable to temperature variations, a weak point in the system is the fiber splice itself. For a high degree of structural integration of the fiber laser the region around the splice is just protected by the recoating material. Thus, a highly resilient splice is of inherent importance. To examine the tensile strength of such a splice an active and a passive fiber of the same geometric dimension (as used in the experimental setup) are spliced together and taken under tensile force up to the point where the splice breaks. By repeating this measurement a Weibull distribution density function and hence, a survival rate for the splice can be retrieved [4]. This approach is used to evaluate and compare the tensile strength for (A) a common splicing procedure and (B) an improved splicing process. The improved splicing procedure is realized by omitting mechanical contact during fiber preparation and thus avoiding micro-cracks in the glass surface which is the main reason for premature breaking of the splice. By doing so, the tensile strength of the splices could be increased from 1.35 N (standard) to 10.16 N (improved) as shown in Figure 9.

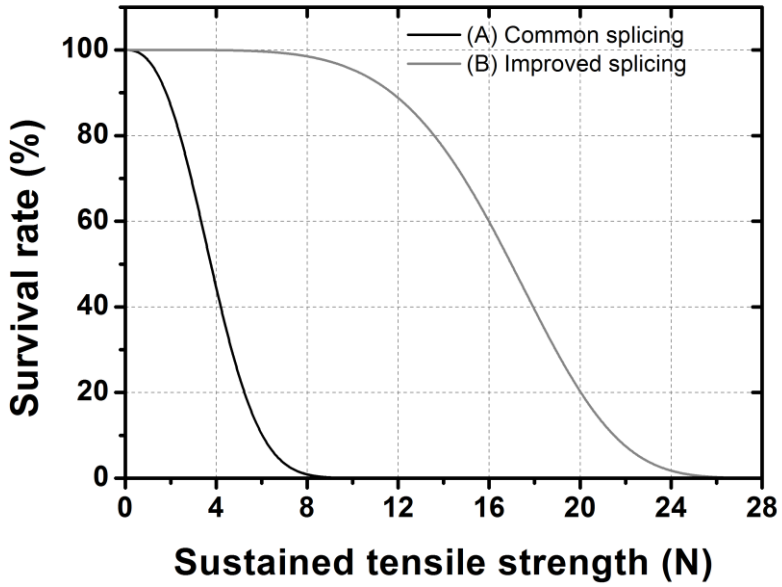

Fig. 9 Weibull distribution of the survival rate of improved high tensile fiber splices and common splices.

4. CONCLUSIONS

The use of lidar to analyze air movement at wind power plants provides some challenges to the laser sources. Thus, the selection of the pulse repetition rate is a compromise between the power scaling to reduce nonlinear effects and the limited processing power of the signal processing system which has to perform many Fourier-transforms per pulse. Within the scope of the presented concepts a range of 5 and 50 kHz pulse repetition rates could be investigated. In the amplifier system in counter-propagation configuration, the SBS-threshold is reached at a pulse peak power of 85 W for pulses with a duration of 220 ns. As opposed to this, the threshold is reached at less than 70 W pulse peak power with the co-propagation configuration. In addition, the slope efficiency of the main amplifier is much higher in the counter-propagation setup.

The propagation length at the system output port should be kept short in order to reduce the influence of non-linear effects on the amplified pulses. This seems to be a strong argument for the usage of the co-propagating system. However, based on the results it could be shown that the counter-propagating setup is preferred in terms of efficiency and SBS threshold for use in lidar systems. The pulse duration has to be scaled to the minimal spatial resolution and the spectral broadening of the pulse, which will be investigated in the near future. In addition, the high stability of the splices and the monolithic design are an advantage when developing compact integrated systems [5].

The indicated limits are based on the attainable results with standard components in the context of cost and availability. In consequence, the shown laser setup is a contribution in terms of costs, efficiency and reliability to improve wind turbine control systems with wind lidar and leads to more effective power plants.

REFERENCES

1. Mark Z. Jacobson and Cristina L. Archer, “ Saturation wind power potential and its implications for wind energy“, PNAS 2012 109 (39) 15679-15684; published ahead of print September 10, 2012, doi:10.1073/pnas.1208993109

2. G. P. Agrawal, Nonlinear Fiber Optics, 4th ed. (Academic Press, 2007).

3. M. González Herráez, K. Y. Song, and L. Thévenaz, “Arbitrary-bandwidth Brillouin slow light in optical fibers,” Opt. Express 14(4), 1395–1400 (2006).

4. A. D. Yablon, Optical Fiber Fusion Splicing, (Springer, 2005)

5. S. Kameyama, T. Ando, K. Asaka, Y. Hirano, and S. Wadaka, "Compact all-fiber pulsed coherent Doppler lidar system for wind sensing," Appl. Opt. 46, 1953-1962 (2007)